Molecular Vision 2005; 11:717-28 <http://www.molvis.org/molvis/v11/a85/>
Received 20 January 2005 | Accepted 29 July 2005 | Published 6 September 2005

Early markers of retinal degeneration in *rd*/*rd* mice

Monica L. Acosta,[1] Erica L Fletcher,[2] Serap Azizoglu,[3] Lisa E Foster,[2] Debora B Farber,[4] Michael Kalloniatis[1]

[1]Department of Optometry and Vision Science, University of Auckland, Auckland, New Zealand; Departments of [2]Anatomy and Cell Biology and [3]Optometry and Vision Sciences, The University of Melbourne, Victoria, Australia; [4]Jules Stein Eye Institute, UCLA School of Medicine, Los Angeles, CA

Purpose: In the *rd*/*rd* mouse, the cell death of rod photoreceptors has been correlated to abnormal levels of the cyclic nucleotide cGMP within photoreceptors. Given that cGMP is required for opening of the cationic channels, there is the possibility that a high cGMP concentration would maintain these channels open, at a high energy cost for the retina.
Methods: We investigated whether cation channels were maintained in an open state in the *rd*/*rd* mouse retina by determining the labeling pattern of an organic cationic probe (agmatine, AGB) which selectively enters cells through open cationic channels. The metabolic activity of the *rd*/*rd* mice was measured by assaying lactate dehydrogenase (LDH) activity in several tissues and Na^+/K^+ATPase activity was measured as a function of development and degeneration of the retina.
Results: AGB neuronal labeling showed a systematic increase consistent with the known neuronal functional maturation in the normal retina. There was a significant higher AGB labeling of photoreceptors in the *rd*/*rd* mouse retina from P6 supporting the possibility of open cationic channels from an early age. There were no changes in the LDH activity of tissues that contain PDE6 or that have a similar LDH distribution as the retina. However, LDH activity was significantly higher in the *rd*/*rd* mouse retina than in those of control mice from birth to P6, and it dramatically decreased from P9 as the photoreceptors degenerated. The predominant LDH isoenzyme changes and loss after degeneration appeared to be LDH5. ATPase activity increased with age, reaching adult levels by P16. Unlike LDH activity, there was no significant difference in Na^+/K^+ATPase activity between control and *rd*/*rd* mice at any age examined.
Conclusions: We conclude that AGB is a useful marker of photoreceptors destined to degenerate. We discard the possibility of a generalized metabolic effect in the *rd*/*rd* mice. However, the elevated LDH activity present before photoreceptor differentiation indicated altered retinal metabolic activity that could not be associated with open cationic channels alone. Therefore, altered metabolic activity as indicated by LDH measurements in the retina appeared to be the earliest sensitive sign of future photoreceptor dysfunction in the *rd*/*rd* mice.

Retinitis pigmentosa (RP) refers to a family of hereditary disorders that are manifested as a gradual loss of photoreceptors and consequently vision. Many genes identified as causally linked to the onset of RP are required for different functions, including phototransduction, maintenance of photoreceptor outer segment integrity, and retinal pigment epithelium retinoid chemistry [1-4]. Despite the identification of possible genetic causes of RP, little information as to the cellular mechanisms that lead to the RP phenotype is available.

A common feature in some forms of autosomal recessive RP is an elevation in the retinal levels of the cyclic nucleotide cGMP, due to specific defects in the cGMP degradation pathway in photoreceptors [5-12]. As cGMP gates cationic channels, elevation of cGMP concentration may contribute to the reduced light sensitivity of rod cells and increased dark current [13-16]. However, an increase in retinal cGMP concentration seems to have a more deleterious effect, as it appears to precede both photoreceptor and inner retina degeneration [10]. Although retarded growth of photoreceptor inner segments is observed after postnatal day 4 [17,18], and swelling of the mitochondria of inner segments is seen by 8 days of life in *rd*/*rd* mice, pyknotic nuclei are first seen at postnatal day 10 [10,19]. Despite such studies and the established elevation of cGMP in some animal models of RP [5,8,10], identifying early biochemical events in the degenerating process may provide useful insights regarding the underlying mechanisms of photoreceptor cell death.

We addressed the issue of identifying the onset of cationic channels opening in the *rd*/*rd* degenerating retinas by examining the entry of agmatine (AGB), a channel-permeable organic cationic probe. AGB enters nonselective cationic channels and has been used as a suitable marker for permeability of ligand-gated channels [20-25]. In the RCS rat retina, photoreceptors destined to degenerate were labeled with AGB before apoptotic markers [26-29], presumably because of the expression of, or the abnormal functioning of cationic channels.

The consequence of elevated cGMP levels in the outer segment of photoreceptors is that these cells would be in a state of constant activity to maintain the influx of sodium and calcium through the cGMP-gated channels; this means that photoreceptors would be maintaining the dark current at a considerable energy cost [30]. This requirement for extraordinary energy would be reflected in the activity of the Na^+/K^+ATPase pump that maintains the ionic gradient, and metabolic enzymes that provide substrates for the tricarboxylic acid cycle.

Correspondence to: Professor Michael Kalloniatis, Department of Optometry and Vision Science, University of Auckland, Private Bag 92019, Auckland, New Zealand; Phone: +64 9 373 7599, ext. 82977; FAX: +64 9 373 7058; email: m.kalloniatis@auckland.ac.nz

Another potential marker of metabolic demand is lactate dehydrogenase (LDH). There is a dramatic alteration in the distribution of LDH isoenzymes in retinal degeneration models [31], with a marked reduction of LDH5 at P7 in the rat retina [32], an age where photoreceptors are not developed and well before anatomical alterations are evident in the RCS rat [33-35]. In addition, a significant decrease in LDH activity has been shown to occur secondary to photoreceptor degeneration in the RCS rat [36,37]. In the *rd*/*rd* mouse model, metabolic anomalies have been demonstrated before anatomical differences. Noell [38] showed an increase in oxygen uptake, glucose utilization and lactic acid production (aerobic) detectable at P8 in the *rd*/*rd* mouse retina, followed by a rapid decrease from P12. The implication of altered metabolic changes at this age is that *rd*/*rd* photoreceptors may have changed their metabolic demand secondary to abnormal cation entry caused by elevated cGMP levels.

The primary lesion of the *rd*/*rd* mice is on the PDE6B gene. PDE6 is found in the retina, and in the brain [39,40]. Studies on the dentate gyrus region of the *rd*/*rd* mice showed a decrease in number of neurons [41] although synaptic plasticity has been related to the activity of PDE5 instead of PDE6 [42]. In another model of retinal degeneration, (the RCS rat), the cause of the retinal degeneration has been associated to a defect in the retinal pigment epithelium (RPE) in a receptor tyrosine kinase that is required for phagocytosis of shed photoreceptor outer segments. However, several studies have shown that there is the possibility of a systemic defect in carbohydrate metabolism in the RCS rats [43,44]. The animals experience difficulty in breeding and a poor muscle reflex [8].

As part of this study we sought to determine if animal models of retinal degeneration also have a systemic metabolic defect and identify early markers in the retina of impending photoreceptor degeneration. Metabolic activity in the *rd*/*rd* mice was probed by determining enzyme activity of LDH in several tissues and Na^+/K^+ATPase in the retina. Photoreceptor cation channel permeability was assessed using an organic cation channel probe (AGB).

METHODS

Animals: All procedures were approved by a University of Melbourne or University of Auckland ethics committee and comply with the Association for Research in Vision and Ophthalmology statement for the use of animals in Ophthalmic and Vision research. Groups of C57BL/6 and *rd*/*rd* mice of several ages were killed by decapitation or cervical dislocation, their eyes removed and the retinas dissected free from the eyecup. In addition to the retina, samples were also taken from the cerebral cortex (somatosensory area), ventricular heart, and skeletal muscle. Tissue samples were homogenized in ice-cold 0.9% (w/v) NaCl in a glass-teflon homogenizer and centrifuged at 5000x g for 5 min at 4 °C. Supernatants were removed, stored on ice, and used for the assays within 30 min post-dissection.

Lactate dehydrogenase activity: The retinas, brain, heart, and skeletal muscle were collected from C57BL/6 and *rd*/*rd* mice at P1, P3, P5, P6, P7, P8, P9, P11, P15, P20, and adult (>P50). Retina samples were prepared by pooling ten retinas from age P3 or younger, eight retinas from ages P5 to P7 and six retinas from all other ages. The heart muscle and skeletal muscle from the hind leg were weighed out, to ensure equal amounts of tissue were used from each animal. Each retinal LDH datum point is the mean value derived from at least six samples. The mean of individual tissue assays was the average of six absorbance measurements. LDH activity was determined using the LDH reagent (Trace Scientific, Victoria, Australia). Tissue samples were diluted to 0.05 mg/ml in 0.9% NaCl and added to the LDH reagent containing: pyruvate (0.6 mM), NADH (0.23 mM) in phosphate buffer (55 mM) at pH 7.5. The change in NADH absorbance over time ΔA/min was measured in a spectrophotometer (Shimadzu UV-2501PC) at 340 nm. The activity of LDH in each sample was calculated and expressed in μmoles/min/mg protein.

Measurement of protein concentration: Protein concentration was measured in a colorimetric reaction using a BCA Protein assay reagent (Pierce, Rockford, IL) and detected in a microplate reader (ELx800, Bio-Tek Instruments Inc., Winooski, VT).

LDH isoenzyme separation: LDH isoenzymes are formed from homo- or heterotetramers of the LDHA and LDHB gene products to generate five isoenzymes. The polypeptides subunits are referred as H and M, which combine to form two pure types of isoenzymes, LDH-1 (H4), and LDH-5 (M4), and three hybrids LDH-2 (H3M), LDH-3 (H2M2), and LDH-4 (HM3) [45]. Native gel electrophoresis was used to separate the five known LDH isoenzymes. This protocol is based on the procedure of Nissen and Schousboe [46] using 1.5% agarose gels (Agarose-1000, Life Technologies) in 25 mM Tris/250 mM glycine (pH 9.5). Electrophoresis was conducted for 90 min at 100 V in a 5 mM Tris, 40 mM glycine, pH 9.5 running buffer. Each sample was run in triplicate with a minimum of five samples per point. Upon completion of electrophoresis, the gel was washed in 0.1 M Tris (pH 8.5) and an LDH staining solution containing lactate (3.24 mg/ml, Sigma, St. Louis, MO), nicotinamide adenine dinucleotide (NAD, 0.3 mg/ml, Sigma), nitroblue tetrazolium (0.8 mg/ml, Sigma) and phenazine methosulfate (0.167 mg/ml, Sigma) dissolved in 0.01 M Tris (pH 8.5) was applied. The Kodak Imaging 1D system was used for visualization and analysis of the gel (Eastman Kodak Company, Rochester, NY). The relative amount of each isoenzyme (LDH1 through LDH5) was determined by quantification of the density of pixels in each isoenzyme band. The cumulative density of the five bands in each sample was calculated and the fraction of individual bands was used to determine the amount of each isoenzyme as a percentage of the whole sample.

Na^+/K^+ATPase activity assay: Retinas from C57BL/6 control mice and *rd*/*rd* mice were used at P4, P8, P16, and adult. Four retinas were pooled for P4 assays, and two retinas were pooled for all other age groups. ATPase activity was measured using a protocol modified from Else and coworkers [47]. Experiments were repeated a minimum of five times. The samples were homogenized in 100 μl 250 mM sucrose, 5 mM EDTA, 20 mM imidazole, (pH 7.4) with a glass-teflon

homogenizer followed by brief sonication. A similar volume of SDS detergent (0.75 mg/ml) was added stepwise under constant mixing and incubated at room temperature for 15 min. ATPase activity was assayed in a solution containing 30 mM L-Histidine, 128 mM NaCl, 4 mM $MgCl_2$, and 20 mM KCl. The ATPase reaction was started by the addition of 25 µl of 30 mM ATP (disodium salt) to 225 µl volume to the other assay constituents, incubating at 37 °C, and was stopped exactly 5 min later with the addition of 0.8 N ice-cold perchloric acid. ATPase activity was also assayed in the presence of 1 mM ouabain to inhibit Na^+/K^+ATPase activity. After centrifugation at 10,000x g for 15 min, the supernatants were reacted with a coloring reagent (10 mg/ml of $(NH_4)_6MO_7O_{24}•4H_2O$, 3.3% H_2SO_4, and 78 mM $FeSO_4•7H_2O$) that reacts with the inorganic phosphate liberated in the ATPase reaction [48]. Na^+/K^+ATPase activity was calculated as the difference in inorganic phosphate liberated in the presence (Mg^{2+}/Ca^{2+}ATPase) and absence (total ATPases) of ouabain and expressed as µmoles PO_4 released per mg protein per hour. Both, Na^+/K^+ATPase and Mg^{2+}/Ca^{2+}ATPase activities were plotted as a function of age.

AGB labeling: AGB enter the cells in a temperature, concentration, and time dependent fashion [49,50], and is a suitable marker of permeability of cationic channels in the verte-

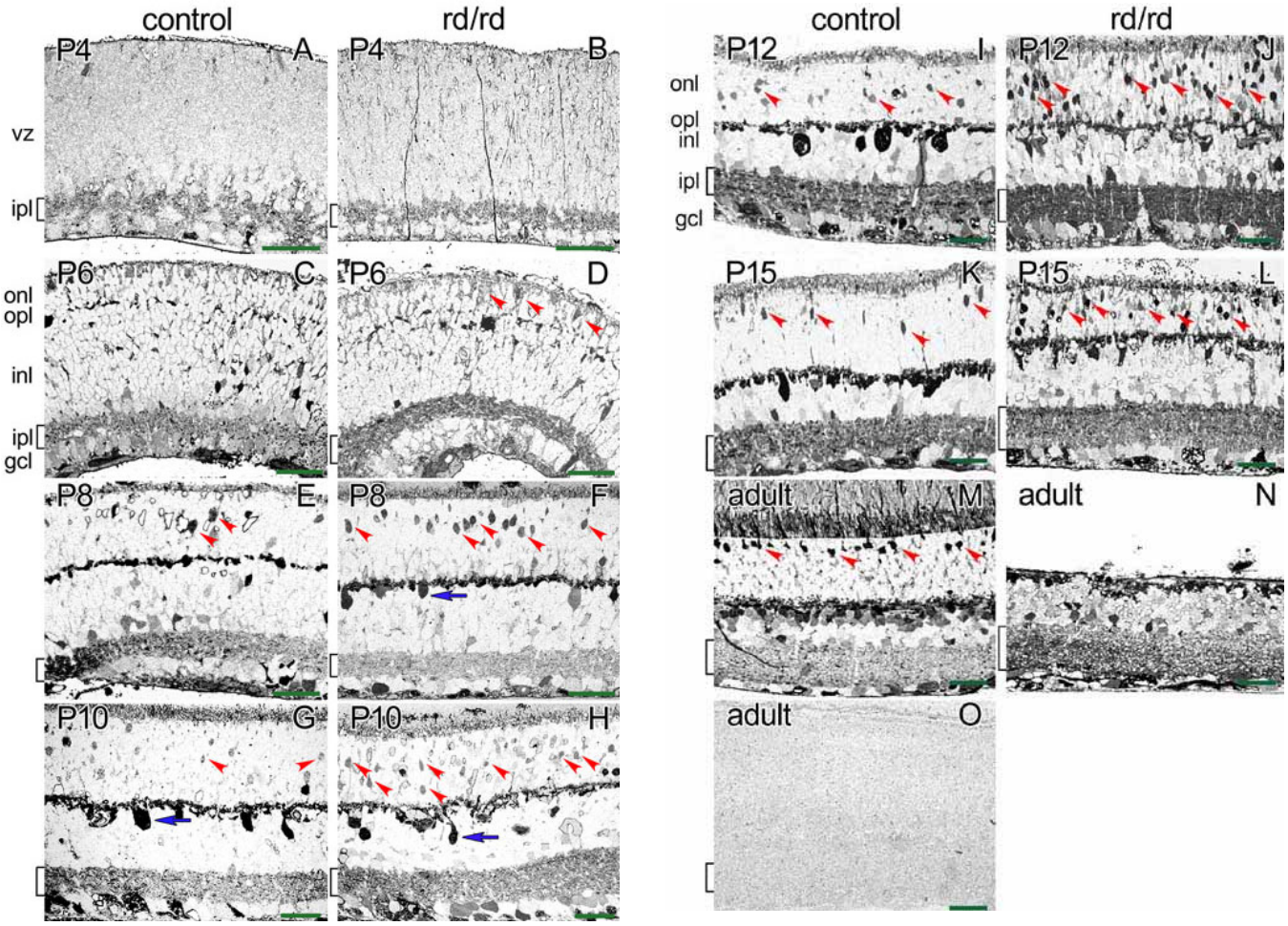

Figure 1. Control and *rd*/*rd* retinas immunolabelled for AGB. **A**,**B**: At P4, light AGB labeling was found in the developing inner plexiform layer. **C**,**D**: At P6, there was light labeling of the inner retina and few of the developing photoreceptor cells. In the *rd*/*rd* mouse, there was increased number of weakly labeled AGB photoreceptor cells. **E**,**F**: At P8, there was occasional labeling of horizontal cells (blue arrow), bipolar cells and the plexiform layers. At this age, an increased number of photoreceptors were strongly labeled in the *rd*/*rd* retina (red arrowheads). **G**,**H**: At P10, control and *rd*/*rd* retinas show labeling of horizontal cells (blue arrow) while in the *rd*/*rd* retinas there was a further increase in the number of labeled cells in the photoreceptor area. **I**,**J**: At P12, there was strong AGB labeling of the inner retina in both control and *rd*/*rd* retinas, while the labeling of the *rd*/*rd* photoreceptors continued to increase. **K**,**L**: At P15, the differences between control and *rd*/*rd* retinas were noticeable in the inner retina and photoreceptor area. **M**,**N**: In the adult, there was strong labeling of the inner retina in the *rd*/*rd* mice with no photoreceptor layer remaining. Panel **O** shows the absence of AGB labeling in an adult retina that was not incubated in the AGB solution. The different retinal layers are indicated in panels **A**, **C**, and **I**. The ventricular zone (VZ), inner plexiform layer (IPL), outer nuclear layer (ONL), outer plexiform layer (OPL), inner nuclear layer (INL), the inner plexiform layer (IPL), and the ganglion cell layer (GCL) are identified. The bracket on the side of each micrograph identifies the inner plexiform layer. The red arrowheads in panels **D**-**M** identify AGB labeled photoreceptors. The scale bar (green bar) corresponds to 20 µm.

brate retina [23]. Incubating the isolated retina under basal conditions (no ligand activation), allows for the assessment of endogenous excitatory drive [23,51] and determination of the activity of cation channels [29]. Retinas from control and *rd*/*rd* mice were dissected and mounted on filter membranes (0.8 μm pore size, Gelman Sciences, Ann Arbor, MI) using a method previously described [23-25,29]. The filter-mounted retinas were incubated in a modified physiological medium containing 100 mM NaCl, 2.5 mM KCl, 26 mM $NaHCO_3$, 1.25 mM NaH_2PO_4, 10 mM dextrose, 2 mM $CaCl_2$, 1 mM $MgCl_2$ [52], to which 25 mM AGB was added. The incubation times varied from 5 to 45 min with optimal detection achieved at 15 min. After the AGB incubation procedure, retinas were fixed in 1% paraformaldehyde/2.5% glutaraldehyde at 4 °C for 1 h. The tissue was dehydrated and embedded in epon resin following procedures previously described in Kalloniatis and Fletcher [53]. Semi-thin (250 nm) serial sections were probed with the AGB antibody provided by Dr. Robert E. Marc (University of Utah, Salt Lake city, UT) and silver-intensified immunogold was used for detection of antibody reactivity. Digital images were acquired with a LEICA DC 500 camera, Twain model V4.1.0.0 mounted on a LEICA DC 500 microscope (Leica Microsystems Ltd., Wetzlar, Germany).

We quantified AGB labeled photoreceptors as a function of age in the outer nuclear layer of retinas drawn with the aid of a camera lucida. Only the central about 2x2 mm area was used for all the quantification to minimize any variation in eccentricity-dependent photoreceptor degeneration. The drawings were also restricted to areas with no signs of conspicuous AGB labeling in the inner retina [23,29]. AGB positive photoreceptor cells were sampled in three separated areas of central retina, which accounted, as closely as possible, for approximately 100,000 μm^2 per retina. The area over which counting was performed was calculated using a calibrated grid placed over the camera lucida drawings. A person blind to the purpose of the experiment performed the drawings and counting. Table 1 outlines the number and age of animals used in the quantification and total area examined in control and *rd*/*rd* mice retinas.

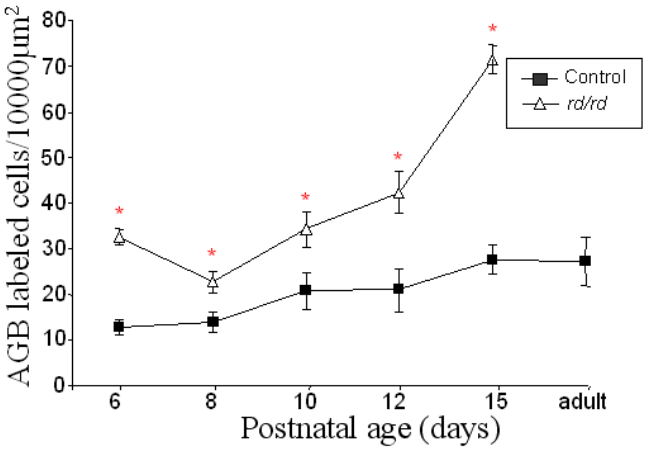

Figure 2. Quantification of AGB labeled photoreceptors as a function of age. The number of AGB labeled cells in the control retina slowly increased through the development of the mouse. At all ages, there was an increased number of AGB labeled *rd*/*rd* photoreceptors per unit area compared with control retina. Significant values are indicated with an asterisk ($p<0.001$).

Statistical analysis: Statistical analysis was performed using one-way analysis of variance (ANOVA) with an α of 0.05 followed by pairwise comparison using Tukey Honestly Significant difference test. All assay data are presented as mean and standard deviation; $p<0.05$ was considered statistically significant.

RESULTS

AGB labeling patterns in the developing retina: We determined the AGB labeling patterns of different age groups in the mouse retina (Figure 1). At P4, no cellular AGB labeling was detected in control (C57BL/6) or *rd*/*rd* retinas, with little labeling of the developing inner plexiform layer. Light labeling of ganglion cells and the inner plexiform layer was observed in the control P6 retina, with rare labeling of amacrine cell somata and the developing photoreceptor cells (Figure 1C). In the *rd*/*rd* mouse, a similar AGB labeling pattern was observed, except for an increased number of AGB labeled photoreceptor cells (Figure 1D, Figure 2). At P8 and in older retinas, AGB immunoreactivity increased in amount and number of cells labeled. There was occasional labeling of horizontal cells and light labeling of bipolar cells and the plexiform layers (Figure 1).

The AGB labeling pattern markedly changed by P10 in

Table 1. Quantitative data of AGB labeling of photoreceptors in C57BL/6 and *rd*/*rd* mouse retinas

	Age					
Control	P6	P8	P10	P12	P15	adult
Number of animals	7	7	6	7	7	8
Number of AGB positive photoreceptors counted	766	1197	1923	1722	2192	2657
Total area of outer nuclear layer examined (μm^2)	601198	836342	953420	1062594	786448	977132
rd/rd	P6	P8	P10	P12	P15	
Number of animals	4	7	8	7	8	
Number of AGB positive photoreceptors counted	1177	1951	3486	2787	3498	
Total area of outer nuclear layer examined (μm^2)	367536	897598	99294	721240	488566	
Labeling ratio (rd/rd:control)	2.5	1.6	1.8	2.4	2.6	

The table show the ages, number of animals and number of AGB positive photoreceptors counted in the outer nuclear layer of control and rd/rd retinas. The ratio of AGB labeled cells in the rd/rd over control retina is indicative of higher AGB entry into the photoreceptors of rd/rd retinas.

both control and *rd*/*rd* retinas. In the control retina there were no major changes in the labeling of the inner retina, except for horizontal cells. In contrast, there was an increase in the number of labeled cells in the *rd*/*rd* retina. At this age, there was dense AGB labeling in the photoreceptors area (Figure 1H). Conspicuous AGB labeling of the inner retina was evident by P12 in both control and *rd*/*rd* retinas (Figure 1I,J). There was an increase in the number of labeled amacrine cell somata. Horizontal cells were intensely labeled, as were the cells in the ganglion cell layer. By P15, the morphology of the control retina was similar to the adult stage although conspicuous labeling of bipolar cells was not evident (Figure 1K). In the adult, the most outstanding differences between control and *rd*/*rd* mice was the absence of the photoreceptor layer and labeling of the inner retina in the *rd*/*rd* mice, consistent with other reports [51,54]. At this stage, the control retina showed an AGB labeling pattern similar to that in the adult rat [29].

Figure 2 shows the proportion of AGB-labeled photoreceptors as a function of age, with the total area sample outlined in Table 1. Although the number of AGB-labeled photoreceptors steadily increased in control retina, the *rd*/*rd* retinas had at all ages a significantly higher number of these labeled cells than the control retinas ($p<0.01$). In the *rd*/*rd* retina, a rapid increase in number of AGB-labeled photoreceptors per

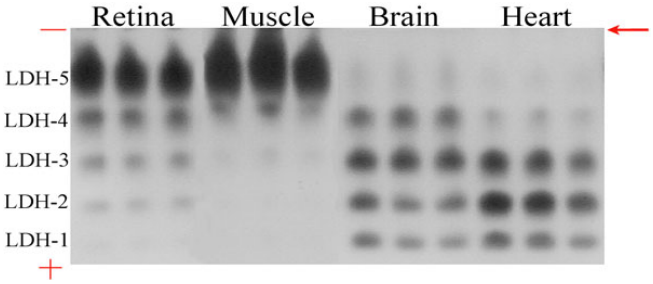

Figure 3. Native gel electrophoresis of LDH isoenzymes in control mouse tissues. The LDH isoenzyme ratio of the brain tissue was similar to ratios found in the aerobic heart tissue that expresses predominantly isoenzymes LDH1-LDH3 and low amounts of the LDH5 isoform. Adult tissues from the anaerobic skeletal muscle express largely the LDH5 isoenzyme. The retina has a similar prevalence of the skeletal muscle-type isoforms in addition to very low amounts of LDH1. The tissue samples were diluted so that equal amounts of LDH activity were loaded into the gel. A volume of 20 µl of each diluted supernatant was added into each electrophoresis gel well. The gel was run at a constant 100 volts from negative to positive for 1.5-2 h or until the bromophenol blue had run out of the gel. Upon the run, the highly colored nitrobluetetrazolium-formazan product localized on zones of LDH activity and the amount of blue color formed was quantitatively related to the level of LDH isoenzyme present. The mobility of the isoenzymes were governed by their individual size and charge. LDH-5, the skeletal muscle isoenzyme migrates the least from the starting point (indicated with an arrow) whereas LDH-1, the heart isoenzyme moves the farthest towards the anode (+) as it has the most positive charge. LDH-2, LDH-3 and LDH-4 migrate towards the anode in order of decreasing anodic mobilities.

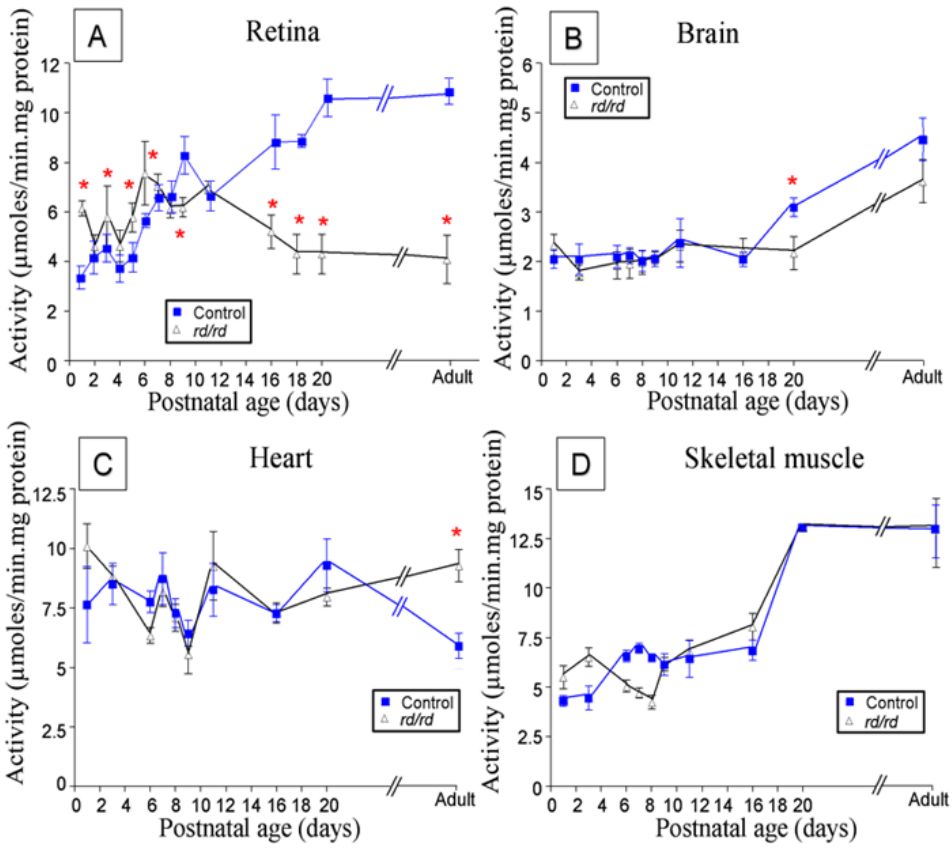

Figure 4. LDH activity in control and *rd*/*rd* tissues as a function of age. **A**: LDH activity in the control mouse retina steadily increased between P5 and P9 followed thereafter by a slow, gradual increment in activity until reaching adult levels. On the contrary, activity in the *rd*/*rd* retina was higher than control before P8 and decreased as photoreceptor cells died. Significantly different values are indicated by an asterisk ($p<0.01$). **B**: An increase in LDH activity was observed in the brain of both control and *rd*/*rd* mice after P16 with significantly different values observed at P20 ($p<0.001$). Total LDH activity was at all ages half the value found for the retina. **C**: LDH activity in the heart of both control and *rd*/*rd* mice was higher than the brain, despite having a similar LDH isoenzyme ratio. LDH activity did not vary through development although the adult value was slightly higher in the control mice ($p<0.01$). **D**: LDH activity in the skeletal muscle of control and *rd*/*rd* mice seemed to be similar to the retina. However, there were no differences between the *rd*/*rd* and control mousee LDH muscle activity.

unit area was observed after P8. By P15, the reduction of the outer nuclear layer width resulted in a ratio of AGB-labeled photoreceptors approximately three times higher than control retina.

LDH in the control mouse: Mammalian LDH exists as five tetrameric isoenzymes referred to as LDH1 through LDH5. The distribution of LDH isoenzymes has been suggested to correlate with different metabolic environments and considering previous work on generalized metabolic dysfunction in models of retinal degeneration, we examined the isoenzyme distribution in mouse heart, skeletal muscle, retina, and brain. As shown in Figure 3, skeletal muscle, which is thought to have high levels of anaerobic metabolism, expressed predominantly the LDH5 isoenzyme. By contrast, heart tissue, which has high levels of aerobic metabolism, expressed predominantly isoenzymes LDH1-3. Although the retina is part of the CNS, it displayed an LDH distribution more akin to muscle than brain. In the retina, LDH5 is the predominant isoenzyme expressed, with decreasing amounts of LDH4 to LDH1. The isoenzyme distribution of brain was similar to heart. These findings are consistent with previous findings [31], in particular that the retina has a greater rate of anaerobic metabolism than any other tissue in the CNS and contains more than three times the lactate per kilogram of tissue compared to brain [55].

Changes in LDH activity during degeneration: To test our hypothesis that the *rd*/*rd* mouse sustain higher metabolic levels than those in control mice, we evaluated their LDH activity as a function of development. As shown in Figure 4A, LDH activity increased in a biphasic manner during development in the control mouse retina. There was a steady increase in LDH activity in the control rat retina, particularly between P6 and P9, a time when photoreceptors begin to form their outer segments, followed by a further increase around eye opening (about P13) and photoreceptor maturation (P20). LDH activity had reached adult levels by P20. In contrast, LDH activity in the *rd*/*rd* mouse was higher than control from P1 to P6 ($p<0.001$, Figure 4A), remained stable between P7 and P8 with values not significantly different from control and decreased thereafter as the photoreceptor cells degenerated reaching LDH activity values encountered in very young retinas.

Figure 4B-D reflects the total LDH activity as a function of age for three other different *rd*/*rd* tissues that either contain PDE6 (brain) and therefore could be affected in the *rd*/*rd* mouse or tissues that have a high content of LDH (heart, muscle). The *rd*/*rd* retina is the only tissue that displayed a consistent increased activity early in development followed by a marked

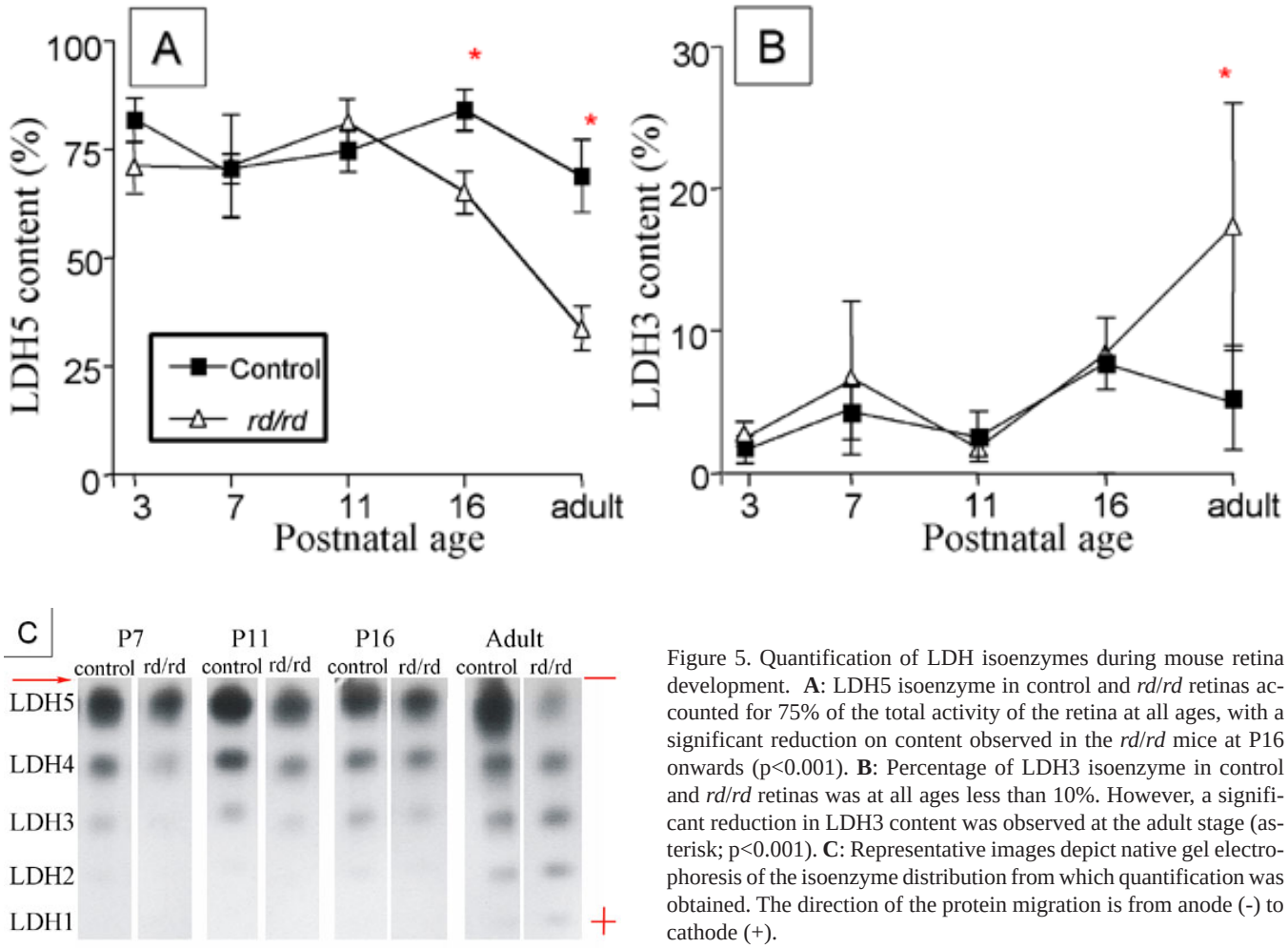

Figure 5. Quantification of LDH isoenzymes during mouse retina development. **A**: LDH5 isoenzyme in control and *rd*/*rd* retinas accounted for 75% of the total activity of the retina at all ages, with a significant reduction on content observed in the *rd*/*rd* mice at P16 onwards ($p<0.001$). **B**: Percentage of LDH3 isoenzyme in control and *rd*/*rd* retinas was at all ages less than 10%. However, a significant reduction in LDH3 content was observed at the adult stage (asterisk; $p<0.001$). **C**: Representative images depict native gel electrophoresis of the isoenzyme distribution from which quantification was obtained. The direction of the protein migration is from anode (-) to cathode (+).

reduction relative to the control retina.

Changes in LDH isoenzyme distribution during degeneration: Changes in LDH activity are often correlated with a shift in expression of LDH isoenzymes. We examined their distribution and quantified the activity of two of the most abundant LDH isoenzymes at five stages of development (Figure 5). There was very little change in the distribution of LDH5 or LDH3 during early developmental ages of the control mouse retina (Figure 5C). In contrast, following eye opening there was a significant decrease in LDH5 content in the *rd*/*rd* mouse (Figure 5A,C). The relative distribution of the LDH5 isoenzyme appeared to parallel the loss of photoreceptors. On the other hand, quantification of LDH3 activity resulted in a small but significant increase ($p<0.01$) in *rd*/*rd* adult retina compared with control values (Figure 5B). We conclude that the overall loss of LDH activity is due to a greater selective loss of the LDH5 isoenzyme.

Changes in Na^+/K^+ATPase during degeneration: It is well known that photoreceptor function has a high metabolic demand. A key enzyme that has been associated with consuming much of this energy is Na^+/K^+ATPase, which is said to account for 50% of energy required by photoreceptors [30]. We evaluated Na^+/K^+ATPase activity in the mouse retina during development and in the degenerating *rd*/*rd* retina. As shown in Figure 6, total ATPase, Mg^{2+}/Ca^{2+}ATPase and Na^+/K^+ATPase activities steadily increased during development. To our surprise, however, there was no difference in activity in degenerating retinas compared with controls at any of the ages examined (Figure 6A-C). The relative change during development of Mg^{2+}/Ca^{2+}ATPase and Na^+/K^+ATPase appeared to be different. In order to emphasize the relative change in the two ATPases, we calculated a ratio plot. Figure 6D shows that Na^+/K^+ATPase underwent a relatively larger change in the early developmental ages, compared with Mg^{2+}/Ca^{2+}ATPase.

DISCUSSION

The results of this study demonstrated elevated cationic channel permeability by P6, well before apoptotic markers and morphological changes are observed at the microscopic level [10,56]. In addition, LDH activity was elevated in degenerating mouse retinas prior to the onset of loss of photoreceptors. Changes in LDH activity were not significantly different in non-retinal tissue. The elevated LDH activity present at birth in the retina was not related to a change in LDH isoenzyme distribution. A sharp decrease in overall LDH activity with a selective reduction of LDH5 was observed after eye opening, well after the onset of photoreceptor death.

AGB labeling occurs earlier than apoptotic markers in the rd/rd *mouse retina:* In other models of photoreceptor degeneration, such as RCS rat retina, AGB labeling of photoreceptors is observed before the visualization of apoptotic cells [26-28], indicating that cationic channel permeability precedes the onset of cell death. In a similar way, we found a significant increase of AGB labeled photoreceptors from P6 in the *rd*/*rd* mouse retina. Normally in phototransduction, activated rhodopsin triggers the activation of transducin, which in turn

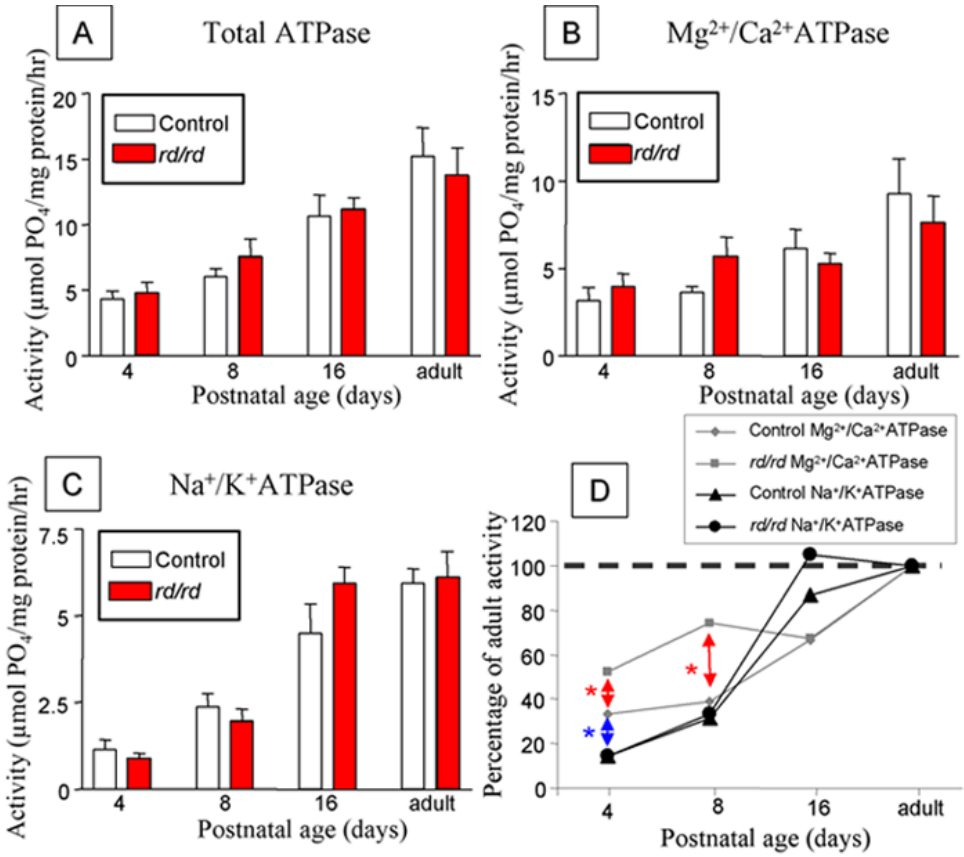

Figure 6. ATPase activity during mouse retina development. **A**: Total ATPase progressively increased through development with no significant differences being present between control and *rd*/*rd* retinas. **B**,**C**: Similar tendency was evident for Mg^{2+}/Ca^{2+}ATPase activity (**B**) and Na^+/K^+ATPase activity (**C**). **D**: The Na^+/K^+ATPase and Mg^{2+}/Ca^{2+}ATPase in control and *rd*/*rd* retinas were compared with the activity of the adult. The plot shows that the relative proportion of Mg^{2+}/Ca^{2+}ATPase activity early in the development of the *rd*/*rd* mice was increased with respect to control values (red double arrows; $p<0.001$) and with respect to Na^+/K^+ATPase activity (blue double arrow; $p<0.01$).

activates phosphodiesterase (PDE), lowering the cGMP levels to close the cationic channels. However, in the *rd*/*rd* mouse, there is a mutation in the gene encoding the β-subunit of rod PDE, resulting in higher cGMP levels in the rod outer segment [7,57]. The increased cGMP content causes the cationic channels in the outer segment to remain open, leading to continued influx of Na^+ and Ca^{2+} ions and induces a sustained dark current that utilizes a high metabolic load [30]. In order to preserve the photoreceptor electrochemical gradient of Na^+, ATP is required. ATP fuels the removal of Na^+ from the photoreceptor, via the action of the Na^+/K^+ATPase. The AGB labeling of photoreceptors destined to degenerate in the *rd*/*rd* mouse retina may indicate open cationic channels (that is, open cyclic nucleotide gated channels), or possibly the expression of other cation permeable channels.

Changes in the pattern of AGB labeling in the *rd*/*rd* retina were also observed in the inner retina, suggesting that altered photoreceptor function is reflected in postneuronal activation. Studies on the permeability of AGB entry in the vertebrate retina [23,24] indicate that AGB labeling of post-receptoral neurons occurs secondary to glutamate receptors activation [23-25] and basal activation [23,24,29,58]. The basal AGB activation pattern reflects overall AGB gating by endogenous activity. It is characterized by a prominent labeling of the outer part of the inner nuclear layer [25,29,58], with occasionally labeled amacrine or ganglion cells. Our observation of altered AGB labeling of the *rd*/*rd* inner retina is in agreement with recent reports that the degenerating retina remodels and establishes excitatory drive [51,54,59-61]. We established that in basal conditions, using 25 mM AGB for longer periods (for example, 15 min) resulted in the labeling of depolarizing bipolar cells; this can be blocked with L-AP4 [52]. The prominent labeling of the outer part of the inner nuclear layer (non-horizontal cells) in the adult control retina is not present in the *rd*/*rd* retina. Such a finding would be expected if "ON" bipolar cell labeling is reduced, as predicted by the finding of the reduced metabotropic glutamate receptor mGluR6 distribution in the outer plexiform layer of *rd*/*rd* retinas [59]. However, the presumed demand to maintain excitatory drive in the remodelled amacrine and ganglion cell layer [51], likely leads to diffuse AGB labeling of the inner nuclear and ganglion cell layers.

There is a higher level of metabolism prior to degeneration in the rd/rd *mouse retina:* Our results indicated that in the control retina, LDH activity increased during development in two phases. There was a steady increase in activity in the control retina between birth and P9, followed by a slow, progressive increase until adulthood. The change in activity, especially between birth and P9 most likely reflects the extent of maturation of retinal structures that occurs prior to eye opening. The mouse retina is relatively immature at birth, consisting of a ganglion cell layer, inner plexiform layer and large neuroblastic layer [10]. The outer plexiform and inner nuclear layers become clearly separated by P4 and photoreceptor outer segments can be observed by P8. The increase in LDH activity observed in the *rd*/*rd* mouse during this early phase could be related to the elevated and increasing cGMP levels relative to protein levels observed from P6 in the *rd*/*rd* retina [5], and decreased cGMP-PDE activity that starts to manifest at P5 [62]. Previous studies [63,64], have shown that synaptogenesis is linked with major changes in metabolism in other regions of the CNS. In particular, LDH activity has been shown to increase during periods of synaptic reorganization in the dentate gyrus following deafferentation [64].

Although the AGB labeling would predict altered metabolic demand from P6, we found a small but significant increase in LDH activity from birth through to P6 in the *rd*/*rd* retina. The increase in LDH activity prior to P6 is consistent with an increase in retinal metabolism prior to the onset of photoreceptor metabolism, and although the activity is not totally consistent with the increase being due to altered photoreceptor metabolic demand alone, is indicative of early altered metabolism in the *rd*/*rd* retina. Rhodopsin is first detected at about P4 with subsequent photoreceptor development and differentiation rapidly occurring in the next few days [10,65-67]. The earliest anatomical difference between the *rd*/*rd* and control mouse is abnormal synaptogenesis at P4 [10] but the first signs of degeneration are observed at P8.

It has not been established if altered energetic metabolism leads to degeneration of the retina. However, the altered LDH enzyme activity is not new to models of retinal degeneration. Graymore [31] published the first reported alteration in LDH distribution in the RCS rat compared to control rat retina. He showed an alteration in the distribution of LDH isoenzymes with a marked reduction of LDH5 at P7, an age where photoreceptors have not attained adult-like morphology in the rat retina and well before anatomical alterations are evident in the RCS rat [31,33-35]. In the *rd*/*rd* mouse model, metabolic anomalies have also been demonstrated before degeneration, and at a similar time to those reported in this study. Several studies [38,68,69], have shown an increase in oxygen uptake, glucose utilization and lactic acid production (aerobic) detectable at P8 in the *rd*/*rd* mouse retina, followed by a rapid decrease from P12. Metabolic substrate concentrations and high energy phosphate compounds do not show major differences between control and *rd*/*rd* mice [70,71], especially between P15 and P20. The changes in oxygen consumption, glucose utilization, and lactic acid production [38] are consistent with altered LDH activity data, and identify an early metabolic dysfunction in the *rd*/*rd* mouse, well before photoreceptor cells die through apoptosis at about P10-P12 in the *rd*/*rd* mouse [56]. The implication of altered metabolic changes at birth is that the genetic mutation leads to altered retinal metabolic function. The chief conclusion that can be drawn from such work is that in two disparate models of retinal degeneration, the RCS rat, caused by a mutation of the tyrosine kinase gene *Mertk* [72,73] and the *rd*/*rd* mouse (caused by a mutation of PDE) [10], both display metabolic anomalies and increased photoreceptor AGB labeling [29] before anatomical or apoptotic markers of impending photoreceptor degeneration.

Is the LDH5 isoenzyme localized within photoreceptors?: It has been proposed that LDH5 is the predominant isoenzyme within glia of the CNS, whereas LDH1 is predominantly

found in neurons [74-76]. This proposition lead to the suggestion that LDH1 is predominantly located within photoreceptors, known to have high use of pyruvate [77]. Consequently, a model was developed for the retina where glucose would be converted to lactate via LDH5 within Müller cells, the lactate transported to photoreceptors where it would be converted to pyruvate via LDH1 and utilized in aerobic metabolism: known as the "lactate shuttle" [75,78,79]. The "lactate shuttle" hypothesis remains controversial [80,81]; however, our previous work has indicated that monocarboxylate transport is important for longer-term retinal function and a range of amino acids are likely shunted into metabolic pools to sustain retinal function [82,83]. Studies on the behavior of LDH isoenzymes at near physiological concentration [84,85] suggest that the activity of LDH isoenzymes may not be as proposed in the lactate shuttle hypothesis. Wuntch's experiments demonstrated that pyruvate inhibition of LDH1 does not occur at concentrations higher than $3.5x10^{-7}$ M, such as those encountered in physiological conditions. Moreover, it has been recently shown that neurons and glia are both net producers of lactate [86]. These observations do not contradict the studies of Bui et al. [83], who observed that when monocarboxylate transporters are blocked, there is a decrease in retinal function as measured by the electroretinogram. Lactate transport inhibition occurs both at the plasma membrane and mitochondrial membrane, opening the possibility that intracellular lactate traffic could be affected. Despite the controversy on the cellular producers of lactate, these studies [87,88] suggest that lactate is a key energy metabolite for retinal neurons, and LDH activity is required for retinal function.

Our observation that the LDH isoenzymes varied considerably between retinal and brain tissue poses the question regarding how the lactate shuttle would operate within the retina. In particular, we observed substantial levels of LDH5 within the retina, and little if any LDH1. It should be noted however, that LDH5 has an equilibrium constant of 1, suggesting that this isoenzyme is just as efficient in producing pyruvate under aerobic conditions as LDH1. Since the oxygen tension in the outer retina is very high [89,90], it is highly probable that the LDH5 equilibrium will be in the direction of pyruvate production. Moreover, the LDH isoenzyme directionality does not seem to apply to physiological concentrations of the enzyme [84,85]. Consequently, in contrast to neurons of the brain that contain LDH1, production of pyruvate or lactate within photoreceptors and Müller cells could be catalyzed by LDH5 under normal metabolic conditions. This suggestion is supported by the distribution pattern of the total LDH activity in the outer retinal layers in both monkey and rabbit retinas [91]. Lowry's work [91] showed that LDH activity in retinal layers is higher in the outer nuclear layer than in the inner retina. It is unlikely that LDH1 alone determines the high activity observed in this layer. In fact, it appears that regulation of LDH5 accounts for the LDH activity of the retina. Several independent studies corroborate this statement: (1) the significant reduction in LDH5 activity in a rat model of photoreceptor degeneration [32,36,37] and (2) LDH5 activity increased in a retinal preparation where the glial metabolism has been impeded [88], suggesting that altered metabolite availability from Müller cells leads to upregulation within neurons. Since LDH5 is the predominant isoenzyme of the mouse retina, it is likely that photoreceptors express this isoform, and that blocking glial metabolism enhances LDH5 activity in the photoreceptors. Further analysis of LDH isoenzyme distribution in the retina is required to support this hypothesis.

ATPase activity in the retina: Na^+/K^+ATPase restores Na^+ and K^+ gradients within photoreceptors and is integral to the maintenance of the photoreceptor dark current. Ames et al. [30] indicated that 41% of oxygen uptake and 58% of glycolysis was consumed by photoreceptor Na^+/K^+ATPase. Moreover, several studies have demonstrated that knockout mice that lack the β2-subunit of Na^+/K^+ATPase, develop photoreceptor degeneration, and that replacing the β2-subunit with a β1-subunit in a "knock-in" experiment ameliorated the degeneration [92-94]. These studies suggest that normal function of Na^+/K^+ATPase is crucial for photoreceptor survival.

We examined Na^+/K^+ATPase activity as a function of development in control and *rd*/*rd* retinas. Following eye-opening, there was a substantial increase in Na^+/K^+ATPase activity in control and *rd*/*rd* retinas. This most likely reflects the increase in retinal function that occurs at this time. The electroretinogram is a gross retinal potential that provides a measure of the response of the retina to light. It is first detected at P12 in the control mouse retina [95]. At this time the rates of glycolysis and oxygen consumption increase by 2.5 fold [96,97]. This roughly coincides with the greatest increase in Na^+/K^+ATPase activity observed.

However, the activity of Mg^{2+}/Ca^{2+}ATPase appeared to be affected early in the development of the *rd*/*rd* mouse retina. The close functional association between PDE activity and Ca^{2+} levels suggest that upregulation of Ca^{2+} ATPases would accompany the degeneration process. Yet, Mg^{2+}/Ca^{2+}ATPase activity was only increased early in the development. It is unlikely that the high Mg^{2+}/Ca^{2+}ATPase activity of the *rd*/*rd* mice at P4 was a consequence of the onset of the degeneration because PDE activity and cGMP levels remain normal at this age [62,98]. Increased cGMP levels and concomitant reduction in PDE activity were first observed at P6 [62,98]. Although there is expanding evidence on the role of the family of plasma membrane Ca^{2+} ATPases (PMCAs) as important participants in maintaining Ca^{2+} export during normal and pathological conditions [99-102], the role of Mg^{2+}/Ca^{2+}ATPase in the *rd*/*rd* retina development remains unclear.

It is intriguing that we found no difference in Na^+/K^+ATPase activity in *rd*/*rd* retinas compared with controls. In particular, Na^+/K^+ATPase activity was unchanged even when photoreceptors were significantly reduced in number in the *rd*/*rd* mouse [71]. It is well known that shifts in metabolism and deafferentation cause major alterations in LDH activity. It is less clear what the relationship is between LDH and levels of aerobic or anaerobic metabolism. We propose that LDH activity is an excellent indicator of photoreceptor function, rather than Na^+/K^+ATPase activity. Wetzel et al. [103] demonstrated that Na^+/K^+ATPase subunits are expressed throughout the retina, and functional Na^+/K^+ATPase is required for main-

taining ion gradients in the inner retina. Our results indicated that there was no preferential higher distribution of ATPase activity in the outer retina.

In summary, we evaluated the use of AGB as a marker of early retinal degeneration, LDH isoenzyme distribution, and activity in control and *rd*/*rd* mouse retinas and other tissues and found that between birth and P8, LDH activity was higher in the *rd*/*rd* mouse retinas than in controls. Together with the observation of high AGB permeation into photoreceptors, this supported the hypothesis of altered metabolism from birth and early dysfunction in cation channel gating of photoreceptors.

ACKNOWLEDGEMENTS

This work was supported by grants from the National Health and Medical Research Council (numbers 145735 and 208950), Retina Australia, and the University of Auckland Staff Research Fund. DBF is the recipient of an RPB Senior Scientist Research Award, and MK holds a professorship funded by the Robert G. Leitl estate. We thank Kerry King for conducting the AGB labeling density counts, Professor Robert Marc for the gift of antibodies and Associate Professor P. Else for providing advice and useful discussion.

REFERENCES

1. Farber DB, Danciger M. Identification of genes causing photoreceptor degenerations leading to blindness. Curr Opin Neurobiol 1997; 7:666-73.
2. van Soest S, Westerveld A, de Jong PT, Bleeker-Wagemakers EM, Bergen AA. Retinitis pigmentosa: defined from a molecular point of view. Surv Ophthalmol 1999; 43:321-34.
3. Baehr W, Liebman P. Visual cascade. In: Encyclopedia of Life Sciences. London: Nature Publishing Group; 2002.
4. Daiger SP. Identifying retinal disease genes: how far have we come, how far do we have to go? Novartis Found Symp 2004; 255:17-36,177-8.
5. Farber DB, Lolley RN. Cyclic guanosine monophosphate: elevation in degenerating photoreceptor cells of the C3H mouse retina. Science 1974; 186:449-51.
6. Lolley RN, Farber DB, Rayborn ME, Hollyfield JG. Cyclic GMP accumulation causes degeneration of photoreceptor cells: simulation of an inherited disease. Science 1977; 196:664-6.
7. Farber DB, Shuster TA. Cyclic nucleotides in retinal function and degeneration. In: Adler R, Farber D, editors. The retina: a model for cell biology studies. Part I. Orlando: Academic Press; 1986. p. 239-96.
8. Chader GJ, Aguirre G, Sanyal S. Studies on animal models of retinal degeneration. In: Tso MOM, editor. Retinal diseases: Biomedical foundations and clinical management. Philadelphia: Lippincott; 1988. p. 80-9.
9. Farber DB, Danciger JS, Aguirre G. The beta subunit of cyclic GMP phosphodiesterase mRNA is deficient in canine rod-cone dysplasia 1. Neuron 1992; 9:349-56.
10. Farber DB, Flannery JG, Bowes-Rickman C. The rd mouse story: seventy years of research on an animal model of inherited retinal degeneration. Prog Retinal Eye Res 1994; 13:31-64.
11. McLaughlin ME, Ehrhart TL, Berson EL, Dryja TP. Mutation spectrum of the gene encoding the beta subunit of rod phosphodiesterase among patients with autosomal recessive retinitis pigmentosa. Proc Natl Acad Sci U S A 1995; 92:3249-53.
12. Danciger M, Blaney J, Gao YQ, Zhao DY, Heckenlively JR, Jacobson SG, Farber DB. Mutations in the PDE6B gene in autosomal recessive retinitis pigmentosa. Genomics 1995; 30:1-7.
13. Nicol GD, Miller WH. Cyclic GMP injected into retinal rod outer segments increases latency and amplitude of response to illumination. Proc Natl Acad Sci U S A 1978; 75:5217-20.
14. Zimmerman AL, Yamanaka G, Eckstein F, Baylor DA, Stryer L. Interaction of hydrolysis-resistant analogs of cyclic GMP with the phosphodiesterase and light-sensitive channel of retinal rod outer segments. Proc Natl Acad Sci U S A 1985; 82:8813-7.
15. Hestrin S, Korenbrot JI. Effects of cyclic GMP on the kinetics of the photocurrent in rods and in detached rod outer segments. J Gen Physiol 1987; 90:527-51.
16. Barabas P, Kovacs I, Kovacs R, Palhalmi J, Kardos J, Schousboe A. Light-induced changes in glutamate release from isolated rat retina is regulated by cyclic guanosine monophosphate. J Neurosci Res 2002; 67:149-55.
17. Caley DW, Johnson C, Liebelt RA. The postnatal development of the retina in the normal and rodless CBA mouse: a light and electron microscopic study. Am J Anat 1972; 133:179-212.
18. Sanyal S, Bal AK. Comparative light and electron microscopic study of retinal histogenesis in normal and rd mutant mice. Z Anat Entwicklungsgesch 1973; 142:219-38.
19. LaVail MM, Sidman RL. C57BL-6J mice with inherited retinal degeneration. Arch Ophthalmol 1974; 91:394-400.
20. Yoshikami D. Transmitter sensitivity of neurons assayed by autoradiography. Science 1981; 212:929-30.
21. Quik M. Inhibition of nicotinic receptor mediated ion fluxes in rat sympathetic ganglia by BGT II-S1 a potent phospholipase. Brain Res 1985; 325:79-88.
22. Kuzirian A, Meyhofer E, Hill L, Neary JT, Alkon DL. Autoradiographic measurement of tritiated agmatine as an indicator of physiologic activity in Hermissenda visual and vestibular neurons. J Neurocytol 1986; 15:629-43.
23. Marc RE. Mapping glutamatergic drive in the vertebrate retina with a channel-permeant organic cation. J Comp Neurol 1999; 407:47-64.
24. Marc RE. Kainate activation of horizontal, bipolar, amacrine, and ganglion cells in the rabbit retina. J Comp Neurol 1999; 407:65-76.
25. Sun D, Rait JL, Kalloniatis M. Inner retinal neurons display differential responses to N-methyl-D-aspartate receptor activation. J Comp Neurol 2003; 465:38-56.
26. Tso MO, Zhang C, Abler AS, Chang CJ, Wong F, Chang GQ, Lam TT. Apoptosis leads to photoreceptor degeneration in inherited retinal dystrophy of RCS rats. Invest Ophthalmol Vis Sci 1994; 35:2693-9.
27. Maslim J, Valter K, Egensperger R, Hollander H, Stone J. Tissue oxygen during a critical developmental period controls the death and survival of photoreceptors. Invest Ophthalmol Vis Sci 1997; 38:1667-77.
28. Valter K, Maslim J, Bowers F, Stone J. Photoreceptor dystrophy in the RCS rat: roles of oxygen, debris, and bFGF. Invest Ophthalmol Vis Sci 1998; 39:2427-42.
29. Kalloniatis M, Tomisich G, Wellard JW, Foster LE. Mapping photoreceptor and postreceptoral labelling patterns using a channel permeable probe (agmatine) during development in the normal and RCS rat retina. Vis Neurosci 2002; 19:61-70.
30. Ames A 3rd, Li YY, Heher EC, Kimble CR. Energy metabolism of rabbit retina as related to function: high cost of Na+ transport. J Neurosci 1992; 12:840-53.
31. Graymore C. Metabolism of the developing retina. 7. Lactic dehydrogenase isoenzyme in the normal and degenerating retina.

A preliminary communication. Exp Eye Res 1964; 3:5-8.
32. Graymore C. Possible significance of the isoenzymes of lactic dehydrogenase in the retina of the rat. Nature 1964; 201:615-6.
33. Fletcher EL, Kalloniatis M. Neurochemical architecture of the normal and degenerating rat retina. J Comp Neurol 1996; 376:343-60.
34. Fletcher EL, Kalloniatis M. Localisation of amino acid neurotransmitters during postnatal development of the rat retina. J Comp Neurol 1997; 380:449-71.
35. Fletcher EL, Kalloniatis M. Neurochemical development of the degenerating rat retina. J Comp Neurol 1997; 388:1-22.
36. Bonavita V, Ponte F, Amore G. Neurochemical studies on the inherited retinal degeneration of the rat. I. Lactate dehydrogenase in the developing retina. Vision Res 1963; 61:271-80.
37. Bonavita V. Molecular and kinetic properties of NAD- and NADP-linked dehydrogenases in the developing retina. In: Graymore CN, editor. Biochemistry of the retina. London: Academic Press; 1965. p.5-13.
38. Noell WK. Aspects of experimental and hereditary retinal degeneration. In: Graymore CN, editor. Biochemistry of the retina. London: Academic Press; 1965. p. 51-72.
39. Shenolikar S, Thompson WJ, Strada SJ. Characterization of a Ca2+-calmodulin-stimulated cyclic GMP phosphodiesterase from bovine brain. Biochemistry 1985; 24:672-8.
40. Taylor RE, Shows KH, Zhao Y, Pittler SJ. A PDE6A promoter fragment directs transcription predominantly in the photoreceptor. Biochem Biophys Res Commun 2001; 282:543-7.
41. Wimer RE, Wimer CC, Alameddine L, Cohen AJ. The mouse gene retinal degeneration (rd) may reduce the number of neurons present in the adult hippocampal dentate gyrus. Brain Res 1991; 547:275-8.
42. Kuenzi F, Rosahl TW, Morton RA, Fitzjohn SM, Collingridge GL, Seabrook GR. Hippocampal synaptic plasticity in mice carrying the rd mutation in the gene encoding cGMP phosphodiesterase type 6 (PDE6). Brain Res 2003; 967:144-51.
43. Ennis S, Pautler E. Expression of the genetic defect associated with inherited retinal dystrophy in the rat. Metab Pediatr Ophthalmol 1979; 3:11-14.
44. Stramm LE, Pautler EL. Glucose uptake by normal and dystrophic rat retinas and ciliary bodies. Exp Eye Res 1980; 30:709-18.
45. Cohen LH, Noell WK. Glucose catabolism of rabbit retina before and after development of visual function. J Neurochem 1960; 5:253-76.
46. Nissen C, Schousboe A. Activity and isoenzyme pattern of lactate dehydrogenase in astroblasts cultured from brains of newborn mice. J Neurochem 1979; 32:1787-92.
47. Else PL, Windmill DJ, Markus V. Molecular activity of sodium pumps in endotherms and ectotherms. Am J Physiol 1996; 271:R1287-94.
48. Fiske CH, Subbarow Y. The colorimetric determination of phosphorous. J Biol Chem 1925; 66:375-400.
49. Dwyer TM, Adams DJ, Hille B. The permeability of the endplate channel to organic cations in frog muscle. J Gen Physiol 1980; 75:469-92.
50. Picco C, Menini A. The permeability of the cGMP-activated channel to organic cations in retinal rods of the tiger salamander. J Physiol 1993; 460:741-58.
51. Marc RE, Jones BW, Watt CB, Strettoi E. Neural remodeling in retinal degeneration. Prog Retin Eye Res 2003; 22:607-55.
52. Edwards FA, Konnerth A, Sakmann B, Takahashi T. A thin slice preparation for patch clamp recordings from neurones of the mammalian central nervous system. Pflugers Arch 1989; 414:600-12.
53. Kalloniatis M, Fletcher EL. Immunocytochemical localization of the amino acid neurotransmitters in the chicken retina. J Comp Neurol 1993; 336:174-93.
54. Marc RE, Jones BW. Retinal remodeling in inherited photoreceptor degenerations. Mol Neurobiol 2003; 28:139-47.
55. Warburg OH. On the metabolism of tumours in the body. In: Warburg OH, editor. The metabolism of tumours [Translated by F. Dickens]. New York: Richard R. Smith, Inc.; 1931. p. 254-70.
56. Portera-Cailliau C, Sung CH, Nathans J, Adler R. Apoptotic photoreceptor cell death in mouse models of retinitis pigmentosa. Proc Natl Acad Sci U S A 1994; 91:974-8.
57. Bowes C, Li T, Danciger M, Baxter LC, Applebury ML, Farber DB. Retinal degeneration in the rd mouse is caused by a defect in the beta subunit of rod cGMP-phosphodiesterase. Nature 1990; 347:677-80.
58. Kalloniatis M, Sun D, Foster L, Haverkamp S, Wassle H. Localization of NMDA receptor subunits and mapping NMDA drive within the mammalian retina. Vis Neurosci 2004; 21:587-97.
59. Strettoi E, Pignatelli V. Modifications of retinal neurons in a mouse model of retinitis pigmentosa. Proc Natl Acad Sci U S A 2000; 97:11020-5.
60. Jones BW, Watt CB, Frederick JM, Baehr W, Chen CK, Levine EM, Milam AH, Lavail MM, Marc RE. Retinal remodeling triggered by photoreceptor degenerations. J Comp Neurol 2003; 464:1-16.
61. Strettoi E, Pignatelli V, Rossi C, Porciatti V, Falsini B. Remodeling of second-order neurons in the retina of rd/rd mutant mice. Vision Res 2003; 43:867-77.
62. Farber DB, Lolley RN. Enzymic basis for cyclic GMP accumulation in degenerative photoreceptor cells of mouse retina. J Cyclic Nucleotide Res 1976; 2:139-48.
63. Borowsky IW, Collins RC. Metabolic anatomy of brain: a comparison of regional capillary density, glucose metabolism, and enzyme activities. J Comp Neurol 1989; 288:401-13.
64. Borowsky IW, Collins RC. Histochemical changes in enzymes of energy metabolism in the dentate gyrus accompany deafferentation and synaptic reorganization. Neuroscience 1989; 33:253-62.
65. Carter-Dawson L, Kuwabara T, O'Brien PJ, Bieri JG. Structural and biochemical changes in vitamin A—deficient rat retinas. Invest Ophthalmol Vis Sci 1979; 18:437-46.
66. Carter-Dawson L, Alvarez RA, Fong SL, Liou GI, Sperling HG, Bridges CD. Rhodopsin, 11-cis vitamin A, and interstitial retinol-binding protein (IRBP) during retinal development in normal and rd mutant mice. Dev Biol 1986; 116:431-8.
67. LaVail MM. Photoreceptor characteristics in congenic strains of RCS rats. Invest Ophthalmol Vis Sci 1981; 20:671-5.
68. Blanks JC, Adinolfi AM, Lolley RN. Photoreceptor degeneration and synaptogenesis in retinal-degenerative (rd) mice. J Comp Neurol 1974; 156:95-106.
69. Blanks JC, Adinolfi AM, Lolley RN. Synaptogenesis in the photoreceptor terminal of the mouse retina. J Comp Neurol 1974; 156:81-93.
70. Lolley RN. Changes in glucose and energy metabolism in Vivo in developing retinae from visually-competent (DBA-1J) and mutant (C3H-HeJ) mice. J Neurochem 1972; 19:175-85.
71. Lolley RN, Racz E. Changes in levels of ATPase activity in developing retinae of normal (DBA) and mutant (C3H) mice. Vision Res 1972; 12:567-71.
72. Gal A, Li Y, Thompson DA, Weir J, Orth U, Jacobson SG, Apfelstedt-Sylla E, Vollrath D. Mutations in MERTK, the hu-

man orthologue of the RCS rat retinal dystrophy gene, cause retinitis pigmentosa. Nat Genet 2000; 26:270-1.
73. D'Cruz PM, Yasumura D, Weir J, Matthes MT, Abderrahim H, LaVail MM, Vollrath D. Mutation of the receptor tyrosine kinase gene Mertk in the retinal dystrophic RCS rat. Hum Mol Genet 2000; 9:645-51.
74. Bittar PG, Charnay Y, Pellerin L, Bouras C, Magistretti PJ. Selective distribution of lactate dehydrogenase isoenzymes in neurons and astrocytes of human brain. J Cereb Blood Flow Metab 1996; 16:1079-89.
75. Poitry-Yamate CL, Poitry S, Tsacopoulos M. Lactate released by Muller glial cells is metabolized by photoreceptors from mammalian retina. J Neurosci 1995; 15:5179-91.
76. Hevner RF, Liu S, Wong-Riley MT. A metabolic map of cytochrome oxidase in the rat brain: histochemical, densitometric and biochemical studies. Neuroscience 1995; 65:313-42.
77. Dawson DM, Goodfriend TL, Kaplan NO. Lactic dehydrogenases: functions of the two types. Rates of synthesis of the two major forms can be correlated with metabolic differentiation. Science 1964; 143:929-33.
78. Tsacopoulos M, Magistretti PJ. Metabolic coupling between glia and neurons. J Neurosci 1996; 16:877-85.
79. Tsacopoulos M, Poitry-Yamate CL, MacLeish PR, Poitry S. Trafficking of molecules and metabolic signals in the retina. Prog Retin Eye Res 1998; 17:429-42.
80. Chih CP, Lipton P, Roberts EL Jr. Do active cerebral neurons really use lactate rather than glucose? Trends Neurosci 2001; 24:573-8.
81. Dienel GA, Hertz L. Glucose and lactate metabolism during brain activation. J Neurosci Res 2001; 66:824-38.
82. Bui BV, Kalloniatis M, Vingrys AJ. Retinal function loss after monocarboxylate transport inhibition. Invest Ophthalmol Vis Sci 2004; 45:584-93.
83. Bui BV, Vingrys AJ, Wellard JW, Kalloniatis M. Monocarboxylate transport inhibition alters retinal function and cellular amino acid levels. Eur J Neurosci 2004; 20:1525-37.
84. Wuntch T, Chen RF, Vesell ES. Lactate dehydrogenase isozymes: kinetic properties at high enzyme concentrations. Science 1970; 167:63-5.
85. Wuntch T, Chen RF, Vesell ES. Lactate dehydrogenase isozymes: further kinetic studies at high enzyme concentration. Science 1970; 169:480-1.
86. Winkler BS, Starnes CA, Sauer MW, Firouzgan Z, Chen SC. Cultured retinal neuronal cells and Muller cells both show net production of lactate. Neurochem Int 2004; 45:311-20.
87. Zeevalk GD, Nicklas WJ. Lactate prevents the alterations in tissue amino acids, decline in ATP, and cell damage due to aglycemia in retina. J Neurochem 2000; 75:1027-34.
88. Acosta ML, Kalloniatis M. Short- and long-term enzymatic regulation secondary to metabolic insult in the rat retina. J Neurochem 2005; 92:1350-62.
89. Ahmed J, Braun RD, Dunn R Jr, Linsenmeier RA. Oxygen distribution in the macaque retina. Invest Ophthalmol Vis Sci 1993; 34:516-21.
90. Yu DY, Cringle SJ, Alder V, Su EN. Intraretinal oxygen distribution in the rat with graded systemic hyperoxia and hypercapnia. Invest Ophthalmol Vis Sci 1999; 40:2082-7.
91. Lowry OH, Roberts NR, Lewis C. The quantitative histochemistry of the retina. J Biol Chem 1956; 220:879-92.
92. Magyar JP, Bartsch U, Wang ZQ, Howells N, Aguzzi A, Wagner EF, Schachner M. Degeneration of neural cells in the central nervous system of mice deficient in the gene for the adhesion molecule on Glia, the beta 2 subunit of murine Na,K-ATPase. J Cell Biol 1994; 127:835-45.
93. Molthagen M, Schachner M, Bartsch U. Apoptotic cell death of photoreceptor cells in mice deficient for the adhesion molecule on glia (AMOG, the beta 2- subunit of the Na, K-ATPase). J Neurocytol 1996; 25:243-55.
94. Weber P, Bartsch U, Schachner M, Montag D. Na,K-ATPase subunit beta1 knock-in prevents lethality of beta2 deficiency in mice. J Neurosci 1998; 18:9192-203.
95. Rohrer B, Korenbrot JI, LaVail MM, Reichardt LF, Xu B. Role of neurotrophin receptor TrkB in the maturation of rod photoreceptors and establishment of synaptic transmission to the inner retina. J Neurosci 1999; 19:8919-30. Erratum in: J Neurosci 2000; 20:2072.
96. Graymore C. Metabolism of the developing retina. I. Aerobic and anaerobic glycolysis in the developing rat retina. Br J Ophthalmol 1959; 43:34-9.
97. Graymore C. Metabolism of the developing retina. III. Respiration in the developing normal rat retina and the effect of an inherited degeneration of the retinal neuroepithelium. Br J Ophthalmol 1960; 44:363-9.
98. Abramson DH, Piro PA, Ellsworth RM, Kitchin FD, McDonald M. Lactate dehydrogenase levels and isozyme patterns. Measurements in the aqueous humor and serum of retinoblastoma patients. Arch Ophthalmol 1979; 97:870-1.
99. Lolley RN, Farber DB. Abnormal guanosine 3', 5'-monophosphate during photoreceptor degeneration in the inherited retinal disorder of C3H/HeJ mice. Ann Ophthalmol 1976; 8:469-73.
100. Brandt PC, Sisken JE, Neve RL, Vanaman TC. Blockade of plasma membrane calcium pumping ATPase isoform I impairs nerve growth factor-induced neurite extension in pheochromocytoma cells. Proc Natl Acad Sci U S A 1996; 93:13843-8.
101. Garcia ML, Strehler EE. Plasma membrane calcium ATPases as critical regulators of calcium homeostasis during neuronal cell function. Front Biosci 1999; 4:D869-82.
102. Krizaj D, Demarco SJ, Johnson J, Strehler EE, Copenhagen DR. Cell-specific expression of plasma membrane calcium ATPase isoforms in retinal neurons. J Comp Neurol 2002; 451:1-21.
103. Wetzel RK, Arystarkhova E, Sweadner KJ. Cellular and subcellular specification of Na,K-ATPase alpha and beta isoforms in the postnatal development of mouse retina. J Neurosci 1999; 19:9878-89.

The print version of this article was created on 8 Sep 2005. This reflects all typographical corrections and errata to the article through that date. Details of any changes may be found in the online version of the article.